

Amorphous magnetism in iron-boron systems: First-principles real-space tight-binding LMTO study

A. M. Bratkovsky*

*Interdisciplinary Research Centre in Superconductivity,
University of Cambridge, Madingley Road, Cambridge CB3 0HE, United Kingdom*

A. V. Smirnov

Computer Centre, Kurchatov Institute, 123182 Moscow, Russia
(Received 1 March 1993; revised manuscript received 21 May 1993)

We have performed *ab initio* spin-polarized self-consistent calculations of the electronic structure and magnetic moments in the series of the $\text{Fe}_{100-x}\text{B}_x$ glasses ($0 < x < 60$) with the real-space tight-binding LMTO method. Realistic atomic models consisting of 500 to 864 atoms in a cubic box with periodic boundary conditions were constructed with the use of the Monte Carlo method. The systems studied show itinerant magnetism with the net magnetic moment on iron sites, $\bar{\mu}$, saturating at the maximum value in a region of a (hypothetical) amorphous iron. The iron magnetic moment decreases upon dilution with boron atoms with *no* maximum on the compositional dependence of $\bar{\mu}$. The calculated distribution of the iron moments is *narrow* with the width decreasing towards the boron-rich end of the series. The magnetovolume effect is shown to be noticeable in iron-rich glasses, declining with increasing boron content. No evidence of a tendency to form the spin-glass state has been found in iron-rich borides.

The transition-metal borides have high glass-forming ability and a number of properties of technological and fundamental interest. They have been extensively studied experimentally and reveal unique magnetic properties,¹⁻³ Invar behavior,⁴ strong magnetovolume effect,⁵ high hardness, and high conductivity. The magnetic behavior of transition-metal- (TM-) based glasses is a challenging problem in condensed matter physics which is as yet a matter of controversy and debate both in experiment and theory. Rather intriguing is the behavior of iron-rich glasses where nontrivial magnetic ordering and the instability of the 3d magnetic moment is discussed in the literature.⁵ As regards the experimental situation for the $\text{Fe}_{100-x}\text{B}_x$ metallic glasses, the iron-rich systems are difficult to stabilize and experimental data for $x < 15$ at. % B are rather scarce and ambiguous. A survey of previous experimental data by Cowlam and Carr⁶ shows that some sets of data probably indicate a maximum on the compositional dependence of the net Fe magnetic moment $\bar{\mu}$ at $x \simeq 20$, whereas other data show an almost linear growth of $\bar{\mu}$ with decreasing x up to the value which is nearly equal to that of bcc Fe. They concluded that the linear variation of the magnetic moment with composition is most probably correct, which implies pure amorphous iron will be characteristically ferromagnetic, with high net moment $\bar{\mu}=2.24\mu_B$. Their analysis also showed that the moment values for thin films appear consistently lower by about 15% than those obtained for melt-spun samples. It is well known that amorphous thin films can be prepared by sputtering onto a cooled substrate for a wider compositional range than by the melt-spinning technique. This is believed to be due to much higher quenching rates achieved in

the sputtering technique, so that many more metastable configurations might be frozen in. It may indeed lead to different properties of the samples produced by both methods but little is known on the influence of quenching rate on the structure of metallic or even conventional glasses.⁶

Theoretical attempts to understand amorphous magnetism in iron-based systems include the semi-empirical Hubbard model^{7,8} and the supercell local-density-approximation (LDA) calculations.^{10,11} The former predicts the maximum value for the net magnetic moment at $x \simeq 20$ and $\bar{\mu} \simeq 1\mu_B$ for *a*-Fe, whereas the latter indicates a high value for the magnetic moment in pure amorphous iron [$\bar{\mu}=(2.3-2.46)\mu_B$], and a possibility of a spin-glass behavior has also been discussed.¹²

To gain more insight into the electronic structure and magnetic behavior of the Fe-B glasses we have undertaken extensive LDA calculations of the amorphous magnetism of the $\text{Fe}_{100-x}\text{B}_x$ systems for the compositional interval $0 < x < 60$ within the first-principles real-space tight-binding (TB) LMTO method¹³ in combination with the recursion method.¹⁴ It is worth mentioning that for tight-binding Hamiltonians real-space methods, such as the recursion method (RM) of Haydock *et al.*, have a workload proportional to the size of the system¹⁴ instead of the cubic proportionality of the usual band-structure supercell methods where self-consistency is usually achieved in one k point.^{10,11} The effects of cluster size, number of "exact" recursion coefficients, and termination of the continued fraction are well understood and the accuracy of the method is well controlled. In our studies we have used big clusters consisting of 500-864 atoms constructed by the Monte Carlo method

as described elsewhere^{15,16} which reproduce fairly well the high-resolution diffraction data. Our recent TB-LMTO calculations of Ni-B, Fe-B, and Zr-Be glasses are in very good agreement with photoemission and low-temperature data showing the reliability of the method in studies of paramagnetic^{17,18} and spin-polarized electron density of states in transition-metal glasses.¹⁸

In constructing *ab initio* tight-binding Hamiltonians we have followed the method of Andersen and Jepsen.¹³ The linear muffin-tin orbitals (LMTOs) χ_{RL} are the solutions of the Laplace equation beyond the muffin-tin spheres at sites R and they have long-range tails. Consequently the overlap and Hamiltonian matrices of the LMTO method¹⁹ are long ranged and determined by the so-called structure constants $S_{R'L'RL}^0$. S^0 's are upper bounded in k space; therefore, one can “screen” them by a simple unitary transformation, changing the power-law decay with distance to a rapid exponential decay:¹³

$$S^\alpha = S^0(1 + \alpha S^\alpha) = \frac{1}{\alpha} \left(\frac{1}{\alpha} - S^0 \right)^{-1} \frac{1}{\alpha} - \frac{1}{\alpha}. \quad (1)$$

The transformation is defined by the chosen parameter set of “screening” constants α which allows one to construct both the “most localized” and the “nearly orthonormal” (NO) representation required for the use with the recursion method. In our calculations we have used the *spd* set of screening parameters¹³ ($\alpha_s = 0.34850$, $\alpha_p = 0.05303$, $\alpha_d = 0.01071$, $\alpha_{l>2} = 0$) for Fe sites and the *sp* set ($\alpha_s = 0.28723$, $\alpha_p = 0.02582$, $\alpha_{l>1} = 0$) for B sites. The overlap and Hamiltonian matrices of the TB-LMTO method were expressed through the *two-center* Hamiltonian h^α :

$$h^\alpha = c^\alpha - E_\nu + \sqrt{d^\alpha} S^\alpha \sqrt{d^\alpha}. \quad (2)$$

In practice, we have performed the construction of the NO representation starting from the most localized TB Hamiltonian which is particularly short ranged, and then transforming it to the NO γ representation:²⁰

$$H^\gamma = E_\nu + h^\gamma = E_\nu + h^\alpha - h^\alpha o^\alpha h^\alpha + \dots \quad (3)$$

This atomic-sphere-approximation (ASA) form of the orthonormalized Hamiltonian was used in the present work with the expansion truncated after the third term (which is of *second order* in $E - E_\nu$, where the E_ν 's have been chosen at the centers of the bands). The density of states has been found by the recursion method¹⁴ with the Hamiltonian H^γ (3) and a band edge estimate after Beer and Pettifor.²¹ We use the entire 864-atom cluster for *a*-Fe and 500-atom clusters for other systems to construct the continued fractions needed for the recursions thus suppressing the finite-size effects. We have generated a sequence of $L_s = L_p = 9$ and $L_d = 20$ pairs of continued fraction coefficients (CFC's) for *s*, *p*, and *d* states, respectively. Recently we have applied the method in studies of the paramagnetic density of states (DOS) of Ni-B, Fe₈₀B₂₀, and Zr-Be glasses^{17,18} and the spin-polarized calculations of *a*-Fe₈₀B₂₀ and pure *a*-Ni.¹⁸ Full details of the present implementation are given in

Ref. 18. In the present study of Fe-B glasses we normally have used the moments of the DOS averaged over about 10 atoms of the given element. The use of up to 50 atoms for the construction of a self-consistent potential did not alter the results. The “screened” structure constants S^α were found from Eq. (1) by direct inversion of subclusters containing about 20 nearby atoms around each site with account being taken for the periodic boundary conditions. It is worth mentioning that an approximate way of calculating S^α leads to substantial errors in the DOS shape.²⁰ Due to complete separation of atomic potential parameters taken as an average for the atoms of a given sort, from the structure constants in Eq. (3), all the information about the local coordination of the given atoms is fully preserved. It allows one to perform an accurate estimate of the distribution of local magnetic moments, etc.

The *a*-Fe₈₀B₂₀ is a typical metallic glass extensively discussed in the literature and, therefore, we will refer the properties of the Fe_{100-x}B_x glasses to this particular system. It demonstrates a generic picture of the electronic properties for the TM-*M* glasses. It retains the main features of the DOS shape of crystalline counterparts^{22,23} apart from some washing out under amorphization. This leads us to believe that the stability and magnetic properties of these glasses are analogous to crystalline counterparts where they are determined by both B *p*-B *p* and Fe *d*-B *p* interactions as described by Gelatt *et al.*²⁴ As the transition-metal host is diluted by boron the *d*-*d* bonding becomes weaker, but simultaneously *d* states interact with metalloid *s* and *p* states forming bonding and antibonding hybrids which can be more effective in bonding than the parent states.^{22,24}

The double-peak DOS, shown for Fe_{100-x}B_x glasses in Fig. 1, corresponds to the *d* band that basically divides the spectrum into lower bonding and upper nonbonding states. The important aspect is that B keeps only about one *s* electron in all systems studied, whereas the number of B *p* electrons is as large as approximately 1.5.^{18,20} It would be expected in a naive picture of ionic bonding that B is left with its two *s* electrons after donating his *p* electron to the transition metal.²⁰ On the contrary, the picture is a strongly covalent one, where B *s* states are split up into an occupied bonding part due to interactions with Fe *s* and *d* orbitals. Fe *d* and B *p* orbitals form a strong bond which results in a large occupancy of B *p* states.^{18,20} Thus, the DOS in the Fe₈₀B₂₀ glass shown in Fig. 1(c) has the -0.5 Ry peak in B *p* states and a high occupancy of B *p* states. Our ferromagnetic DOS [Fig. 1(c)] has a strong occupied peak at -0.07 Ry with a left satellite peak at -0.22 Ry. The B *sp* and Fe *s* states produce a shoulder at 0.40 – 0.48 Ry below the Fermi level. This is in close correspondence with the results of high-resolution UV photoemission, Auger electron, and energy-loss spectroscopy.²⁵ Above the Fermi energy we have obtained the empty minority spin band peak which lies at $+0.07$ Ry ($+1$ eV) and should be observable by inverse photoemission. It is worth noting that the Hubbard-model calculations of the Fe₈₀B₂₀ glass⁸ give only one smooth peak on the DOS in contradiction with experiment.²⁵

Comparing the spin-polarized DOS with the paramagnetic DOS,¹⁸ we can conclude that the iron *d* bands split with some shape changes in the minority spin bands owing to the mechanism of covalent magnetism:^{9,22} Namely, the B *p* band does not follow a splitting of the Fe *d* band, which increases the energy difference between these states and those of the minority *d* band. The Fermi level is pinned just above the majority spin band and the difference in occupancies of the majority and minority states vanishes when approaching the boron-rich end of the series (Fig. 1). The actual value of the net moment in *a*-Fe₈₀B₂₀ is $\bar{\mu} = 2.10\mu_B/\text{Fe}$, with the individual values distributed in the interval $(1.5\text{--}2.5)\mu_B/\text{Fe}$. This value of the net iron moment is slightly lower than the previous estimate $\bar{\mu} = 2.2\mu_B/\text{Fe}$ Ref. (20) obtained from the paramagnetic DOS with the generalized Stoner

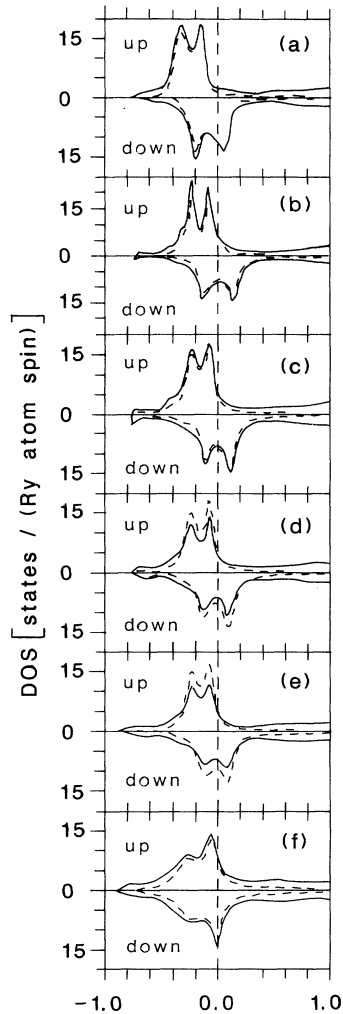


FIG. 1. Ferromagnetic density of states of $\text{Fe}_{100-x}\text{B}_x$: (a) $x = 0$, $\rho = 7.90 \text{ g/cm}^3$; (b) $x = 10$, $\rho = 7.44 \text{ g/cm}^3$; (c) $x = 20$, $\rho = 7.29 \text{ g/cm}^3$; (d) $x = 25$, $\rho = 7.21 \text{ g/cm}^3$; (e) $x = 34$, $\rho = 7.07 \text{ g/cm}^3$; and (f) $x = 50$, $\rho = 6.75 \text{ g/cm}^3$. Solid lines: total DOS per atom; dashed lines: partial DOS of the Fe *d* electrons per Fe atom. Note that partial DOS's of Fe and B contribute to total DOS in accordance with factors $100 - x$ and x .

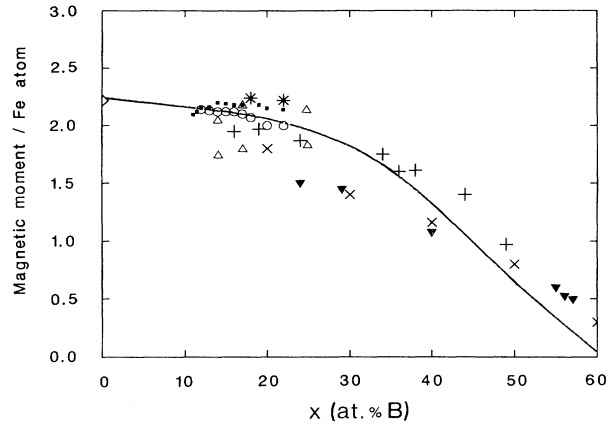


FIG. 2. Compositional dependence of the net iron moment (line). Experimental points: \circ Ref. (3), \triangle Ref. (5), \square Ref. (26), $*$ Ref. (29), $+$ Ref. (27), \times Ref. (28), and ∇ Ref. (30). Diamond indicates the value of the moment in bcc Fe. Two sets of data Ref. (5) obtained by different methods are indicated by the same symbol.

model and is substantially bigger than the supercell result $\bar{\mu} = 1.67\mu_B/\text{Fe}$.¹⁰ There is a substantial scatter in experimental data on the net Fe moment (Fig. 2) with the averaged value of $2.03\mu_B/\text{Fe}$, which is close to our calculated value of $2.10\mu_B/\text{Fe}$. The boron sites acquire a small negative moment ($\sim -0.1\mu_B/\text{B}$) in all systems studied. The calculated DOS at the Fermi level, $N(0)$, is 11 states/(Ry atom), which is close to the generalized Stoner estimate of 15 states/(Ry atom).²⁰ The experimental estimate is 38 states/(Ry atom) Ref. (31) and shows rather unexpected strong itinerant magnetic behavior for the Fe-B glass and this cannot be fully attributed to the electron-phonon mass enhancement which amounts to a factor of 2.²⁰

To investigate the magnetovolume effect we have displayed the distribution of the moments on Fe sites versus the volumes V of circumscribed Voronoi polyhedra for $\text{Fe}_{80}\text{B}_{20}$ and $\text{Fe}_{50}\text{B}_{50}$ in Fig. 3. The sites were taken close to the center of the cluster. The scatter of the $\mu = \mu(V)$ is large in $\text{Fe}_{80}\text{B}_{20}$ but the data collected in Fig. 3 certainly show a correlation of the bigger moments belonging to the sites with lower density, close to the results of the supercell and Hubbard-model calculations for *a*-Fe.^{11,32} The compositional tendency we have found is very interesting: With increasing dilution by boron the local magnetic moments become insensitive to the local volume. It correlates with the narrowing of the moment distribution with an increase in the boron content (Fig. 4). Because of uncertainty in the density data for Fe-B glasses Fig. 3 suggests a reliable estimate of the variation of the net iron moment with density. We have also calculated the magnetovolume effect in a pure *a*-Fe at different densities, and found almost the same correlation: Higher density and lower net magnetic moment corresponds to a lower magnetovolume effect. At the density $\rho = 9.1 \text{ g/cm}^3$ our model *a*-Fe almost loses the magnetic moment; this also takes place in crystalline fcc Fe at this density.³³

Competition between ferromagnetic splitting of the Fe *d* states and covalent Fe *d*-B *p* bonding determines the

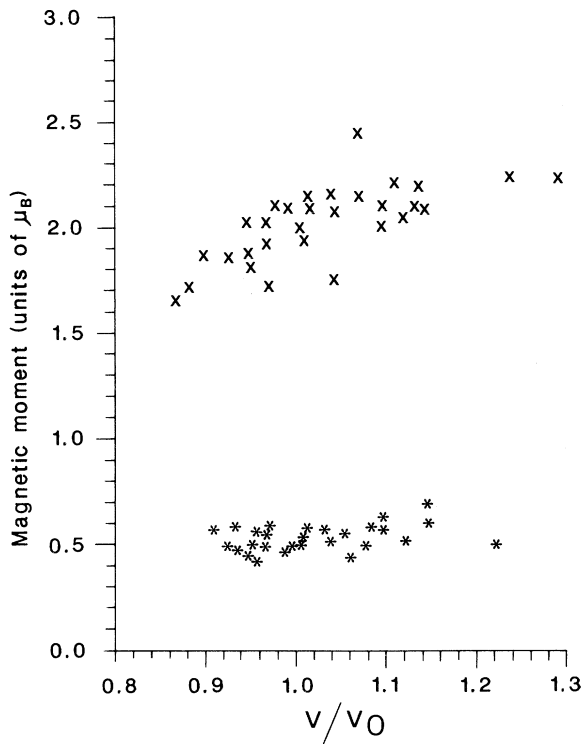


FIG. 3. Magnetovolume effect: (x) $\text{Fe}_{80}\text{B}_{20}$, $V_0 = 10.67 \text{ \AA}^3$; (*) $\text{Fe}_{50}\text{B}_{50}$, $V_0 = 8.20 \text{ \AA}^3$.

composition dependence of the moment on the TM site as is the case in the crystalline counterparts.^{22,23} The minority spin band is pulled down and the moment on the iron sites rapidly decreases to $\bar{\mu} = 0.53\mu_B/\text{Fe}$ in $\text{Fe}_{50}\text{B}_{50}$ (Figs. 1 and 4). Simultaneously the boron *s* and *p* partial DOS gradually increase their weight in the interval from -0.8 to -0.3 Ry in hybridization with the Fe *d* states. This behavior is easily observed with the present method, whereas the supercell methods usually give rather “spiky” DOS shapes for the *sp* extended states.

The iron-rich glasses represent a matter of controversy both in experiment and theory, mentioned above. In the present TB-LMTO calculations the ferromagnetic splitting and the resulting iron moment is large in $\text{Fe}_{80}\text{B}_{20}$. With more iron content in the system the splitting of the *d* band remains strong with the Fermi level pinned just above the majority spin band, and the iron moment increases up to $\bar{\mu} = 2.12\mu_B/\text{Fe}$ in $\text{Fe}_{90}\text{B}_{10}$ and further to $2.25\mu_B$ in pure *a*-Fe (Figs. 1 and 4). The possibility of large local variations in the Fe moment as a precursor of a local antiferromagnetic coupling could have been signaled by a broad distribution of the iron moments $p = p(\mu)$ (Fig. 4) and the appearance of the sites with negative Fe moments.¹² The distribution of the moments has been analyzed over up to 50 atoms close to the center of the cluster, by calculating the site-projected DOS, and this experiences large variations. The present calculations show that the distribution of the Fe moments in iron-rich Fe-B systems is not broad (Fig. 4). In *a*-

Fe moments are distributed in the interval $(2.0\text{--}2.7)\mu_B$ with a somewhat broader distribution in *a*- $\text{Fe}_{90}\text{B}_{10}$ [$(1.7\text{--}2.6)\mu_B$]. The distribution becomes narrower with increasing boron concentration and decreasing Fe-Fe coordination number, and in *a*- $\text{Fe}_{50}\text{B}_{50}$ the moments are distributed in the narrow interval $(0.4\text{--}0.7)\mu_B$ (Fig. 4). The distribution of iron moments shows that the ferromagnetic state remains stable with respect to local concentration and density fluctuations in an amorphous system. It is worth noting that our method somewhat overestimates this stability while in supercell calculations one finds some small fraction of Fe atoms with flipped spins.¹¹ It is worth noting that our calculations did not allow for the noncollinear components of the moment on Fe to appear. In fact, recent diffraction experiments show that in iron-rich amorphous Fe-B systems there may exist some degree of noncollinearity in the moment configuration³⁴ that would be interesting to investigate further.

Summarizing, we showed that the net moment in amorphous $\text{Fe}_{100-x}\text{B}_x$ systems gradually decreases from its high value in pure *a*-Fe (which is close to that of bcc Fe in agreement with prediction of Cowlam and Carr⁶) and that no tendency toward forming the spin-glass state in iron-rich Fe-B glasses has been found. The net iron moment disappears at about $x = 60$ as a result of increasing B *p*-Fe *d* interactions and decreasing exchange splitting.

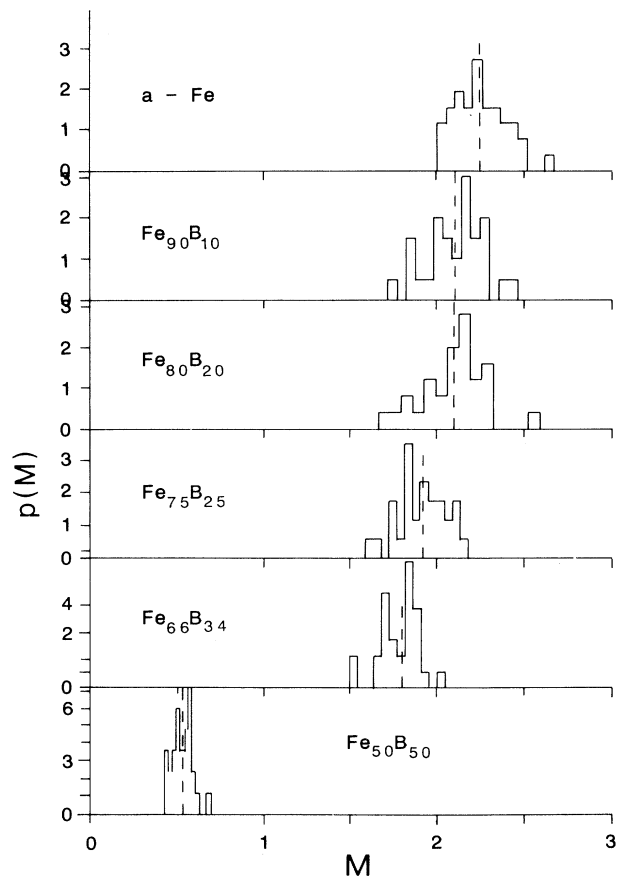


FIG. 4. Distribution of the iron moments in amorphous $\text{Fe}_{100-x}\text{B}_x$.

We showed that a magnetovolume effect is pronounced in systems with a large net iron moment and basically declines with increasing boron content or pressure with a related decrease in the net moment itself. This is believed to be related to ferromagnetic instability and the Invar effect where the LSD calculations provide a realistic explanation of the phenomena.^{33,35,36} It is quite possible

that strong electron correlations might be relevant for this behavior in Fe-based systems and the tight-binding LMTO method provides a natural tool for addressing these questions.³⁷

A.M.B. acknowledges fruitful discussions with V. Heine, N. F. Mott, and D. G. Pettifor.

-
- *Electronic address: amb27@cus.cam.ac.uk
- ¹E.P. Wohlfarth, in *Amorphous Metallic Alloys*, edited by F.E. Luborsky (Butterworths, London, 1983), p. 283.
- ²R. Hasegawa *et al.*, *Appl. Phys. Lett.* **29**, 219 (1976).
- ³R. Hasegawa and R. Ray, *J. Appl. Phys.* **49**, 4174 (1978).
- ⁴K. Fukamichi *et al.*, *J. Magn. Magn. Mater.* **10**, 294 (1979).
- ⁵Z. Xianyu, Y. Ishikawa, S. Ishio, and M. Takahashi, *J. Phys. F* **15**, 1787 (1985); Z. Xianyu, Y. Ishikawa, T. Fukunaga, and N. Watanabe, *J. Phys. F* **15**, 1799 (1985).
- ⁶N. Cowlam and G.E. Carr, *J. Phys. F* **15**, 1109 (1985).
- ⁷U. Krey, U. Krauss, and S. Krompiewski, *J. Magn. Magn. Mater.* **114**, 337 (1992); S. Krompiewski, U. Krey, and H. Ostermeier, *ibid.* **69**, 117 (1987).
- ⁸H. Ostermeier, W. Fembacher, and U. Krey, *Z. Phys. Chem. Neue Folge* **157**, 489 (1988).
- ⁹A.R. Williams, R. Zeller, V.L. Moruzzi, C.D. Gelatt, and J. Kubler, *J. Appl. Phys.* **52**, 2067 (1981).
- ¹⁰Y.-N. Xu, Y. He, and W.Y. Ching, *J. Appl. Phys.* **69**, 5460 (1991); W.Y. Ching and Y.-N. Xu, *ibid.* **70**, 6305 (1991).
- ¹¹I. Turek and J. Hafner, *Phys. Rev. B* **46**, 247 (1992).
- ¹²Y. Kakehashi, *Phys. Rev. B* **43**, 10820 (1991).
- ¹³O.K. Andersen and O. Jepsen, *Phys. Rev. Lett.* **53**, 2571 (1984).
- ¹⁴R. Haydock, V. Heine, and M.J. Kelly, *J. Phys. C* **8**, 2591 (1975).
- ¹⁵A.M. Bratkovsky and A.V. Smirnov, *Phys. Lett. A* **146**, 522 (1990); *J. Non-Cryst. Solids* **117/118**, 211 (1990).
- ¹⁶A.M. Bratkovsky and A.V. Smirnov, *J. Phys. Condens. Matter* **3**, 5153 (1991).
- ¹⁷A.M. Bratkovsky and A.V. Smirnov, *J. Non-Cryst. Solids* **156-158**, 156 (1993).
- ¹⁸A.M. Bratkovsky and A.V. Smirnov, *J. Phys. Condens. Matter* **5**, 3203 (1993).
- ¹⁹O.K. Andersen, *Phys. Rev. B* **12**, 3060 (1975).
- ²⁰H.J. Nowak, O.K. Andersen, T. Fujiwara, O. Jepsen, and P. Vargas, *Phys. Rev. B* **44**, 3577 (1991).
- ²¹N. Beer and D. Pettifor, in *The Electronic Structure of Complex Systems*, edited by P. Phariseau and W.M. Temmerman (Plenum, New York, 1984), p. 769.
- ²²P. Mohn and D.G. Pettifor, *J. Phys. C* **21**, 2829 (1988).
- ²³A.M. Bratkovsky, S.N. Rashkeev, and G. Wendin, *Phys. Rev. B* (to be published).
- ²⁴C.D. Gelatt, A.R. Williams, and V.L. Moruzzi, *Phys. Rev. B* **27**, 2005 (1983).
- ²⁵Th. Paul and H. Neddermeyer, *J. Phys. F* **15**, 79 (1985).
- ²⁶H. Hiroyoshi *et al.*, *Phys. Lett. A* **65**, 163 (1978).
- ²⁷G. Bayreuther *et al.*, *J. Magn. Magn. Mater.* **31-34**, 1535 (1983).
- ²⁸K.H. Buschow and P.G. Engen, *J. Appl. Phys.* **52**, 3557 (1981).
- ²⁹S. Hatta and T. Egami, *J. Appl. Phys.* **50**, 1589 (1979).
- ³⁰T. Stobiecki and F. Stobiecki, *J. Magn. Magn. Mater.* **35**, 217 (1983).
- ³¹M. Matsuura, U. Mizutani, and Y. Yazawa, *J. Phys. F* **11**, 1393 (1981).
- ³²U. Krauss and U. Krey, *J. Magn. Magn. Mater.* **98**, L1 (1991).
- ³³V.L. Moruzzi, P.M. Marcus, and J. Kubler, *Phys. Rev. B* **39**, 6957 (1989).
- ³⁴R.A. Cowley *et al.*, *J. Phys. Condens. Matter* **3**, 9521 (1991).
- ³⁵V.L. Moruzzi, *Solid State Commun.* **83**, 739 (1992).
- ³⁶A.R. Williams, V.L. Moruzzi, C.D. Gelatt, and J. Kubler, *J. Magn. Magn. Mater.* **31-34**, 88 (1983).
- ³⁷O. Gunnarsson *et al.*, *Phys. Rev. B* **39**, 1708 (1989).